269 (1967).
[28]W. K. Chu and D. Powers, Phys. Rev. 187, 478 (1969).
[29]D. I. Porat and K. Ramavataram, Proc. Phys. Soc. (London) 78, 1135 (1961).
[30]H. H. Andersen, H. Simonsen, and H. Sørensen, Nucl. Phys. A125, 171 (1969).
[31]W. Whaling, in *Handbuch der Physik*, edited by S. Flügge (Springer-Verlag, Berlin, 1958), Vol. 34, p. 193.
[32]C. A. Sautter and E. J. Zimmerman, Phys. Rev. 140, A490 (1965).
[33]W. Booth and I. S. Grant, Nucl. Phys. 63, 481 (1965).

PHYSICAL REVIEW B VOLUME 3, NUMBER 11 1 JUNE 1971

Vectorial Photoelectric Effect

R. M. Broudy*
United Aircraft Research Laboratories, East Hartford, Connecticut
(Received 12 January 1971)

Experimental results and their analysis are presented which indicate that the vectorial photoelectric effect originates neither in excitation at the surface nor in pure volume optical absorption, but is a unique combined surface-volume effect which depends only on optical absorption as influenced by the interface. This effect can be phenomenologically regarded as surface-enhanced optical absorption (SEOA) in which, for certain transitions excited by light polarized perpendicular to the surface, optical absorption in the volume near the surface can be increased manifoldly (100 times or more) by the presence of certain surface conditions. Our results show a large decrease in this absorption by controlled modification of the surface for the system investigated, which is single-crystal silicon in ultrahigh vacuum with surfaces oriented parallel to (111), (110), and (100) planes. Photoelectric yields are shown at angles of incidence from 0° to 60° for both polarized and unpolarized light with photon energies in the range 4.6–6.4 eV. Some interface effects are illustrated by photoemission from samples covered with thin (20–100 Å) oxide layers; electron emission is considered in terms of the system silicon-silicon oxide-vacuum. Essential requirements are discussed for a theory of SEOA, the existence of which calls for a reexamination of present approaches to the fundamental theory of photoelectric emission.

I. INTRODUCTION

Photoelectric emission includes several processes: optical absorption by excitation of electrons, motion of the excited carriers, and emission into the collecting medium through the interface. The determination of the spatial and temporal location of these processes, from the earliest days, has been central to the analysis of photoelectric emission, which requires, whatever the mechanism, that conservation of momentum be provided for in the photon-electron interaction.

For many years it was believed, for metals at least, that all processes occurred simultaneously at (within a few angstroms of) the surface. Conservation of momentum in theories[1-4] taking this viewpoint (the "surface photoeffect") is provided at the potential step between the surface and collecting medium (usually vacuum). In such theories, only the component of polarization of the light parallel to the gradient of the potential step, and thus perpendicular to the surface, will cause photoexcitation. And indeed, earlier experimental results[5,6] seemed to be consistent with the qualitative predictions of these theories in that photoelectric measurements showed greater yields for radiation with polarization components perpendicular to the surface. This result was called the "vectorial photoelectric effect" by Ives[6] for reasons which, it is now realized, are not applicable; however, we shall continue with the same terminology, since it has become established by usage. In fact, the difficulties in comparing experiment with theory were not in observing the vectorial effect, but rather in explaining the appreciable yields measured with illumination at normal incidence (necessarily with polarization parallel to the plane of the surface). Normal-incidence yields were generally explained by the introduction of the obvious mechanism of surface roughness.[1] However, the required amount of surface roughness has seemed arbitrary, and there has been no direct correlation available between experiment and theory.

The opposing concept, that optical absorption occurs simply within the volume of the material, was introduced and theoretically developed in 1945 by Fan,[7] who pointed out that momentum would be conserved in volume absorption because electrons move in a periodic potential. Subsequently, the resolution of the surface-volume question was apparently obtained by Thomas and co-workers who, in a series of papers[8-10] on photoelectric emission from thin

films of alkali metals, demonstrated that the optical absorption responsible for their observed photoelectrons occurred within the volume: Observed vectorial effects were considered to be only a consequence of the predicted variation with incidence of classical optical absorption. The subject was reviewed in 1961 and further discussed in 1968 by Meesen, [11] who took the volume point of view.

For semiconductors, the volume origin of photoemission has been generally accepted for some time, both because of experiments on band bending near the surface[12–15] and because yields and energy distributions were found to be consistent with volume excitation within the band structures, [16–19] although considered only for normal-incidence illumination. For metals, much work has established,[20,21] also at normal incidence, that observed photoelectrons originate in the volume.

There has been much less work on vectorial photoemission, perhaps partly because of additional experimental requirements (polarized light and variable incidence), but probably mainly because of the lack of definite knowledge of fundamental processes underlying the effect. Recent observations include vectorial effects on evaporated potassium layers, [22] and on semiconductor photocathodes[23]; in each case, yields were greatest when the polarization was parallel to the plane of incidence, but no definite mechanism for this dependence was established. It has been difficult to relate vectorial experiments to the main body of photoelectric work, since investigations which could reveal the effect were not performed under the highly controlled conditions of surface, crystallography, and ambience which typify the more recent experiments using unpolarized light at normal incidence.

The subject was reopened by Juenker, Waldron, and Jaccodine[24] (hereafter referred to as JWJ), who in 1964 reported the results of experiments in ultrahigh vacuum on carefully controlled polycrystalline molybdenum. Vectorial effects were observed which were much too large to be explained by the conventional volume excitation process, but were also not consistent with any simple surface mechanism; the magnitudes of their vectorial yields were found to depend greatly on the method of sample preparation, with the largest effects being observed for samples which had the least apparent roughness as seen in the optical microscope. Agreement with experimental data was obtained by using a parameter B, which designates the extent to which the component of electric field intensity normal to the surface is favored over the tangential component in effecting photoemission. Their results provided considerable illumination but did not yet allow them to decide between the surface and the volume hypotheses or to determine the physical mechanism involved in the parameter B. They suggest: "Careful measurement of B under controlled experimental conditions would seem to be one way to acquire valuable information concerning the locality of the photoelectric excitation, the nature of the potential variation in which it takes place, and the types of interaction in which the excited electron can take part." The results presented in the present paper provide considerable progress towards the resolution of these questions.

In the work reported here, [25] evidence has been obtained for the existence of a unique phenomenon underlying vectorial photoelectric emission, which, our results indicate, is due neither to excitation at the surface nor to pure volume absorption. Rather, it is a combined volume-surface effect which is due *only* to the fact that volume optical absorption is influenced by conditions at the interface (and not due to a large number of other possibilities, many of which were suggested by JWJ, such as: carrier transport effects, anisotropy of the excitation, crystallographic selection rules, intercrystallite barrier effects, etc.), where the terms "surface" and "interface" are used *only in the strict sense* to refer to the angstrom-sized transition region. The effect can be regarded phenomenologically as surface-enhanced optical absorption (SEOA) in which, for certain transitions excited by light polarized perpendicular to the surface, optical absorption (only for these transitions) in the volume near the interface can be increased manifoldly (as much as 100 times or more) by the presence of proper surface conditions. It appears that band structures near the interface are similar to those

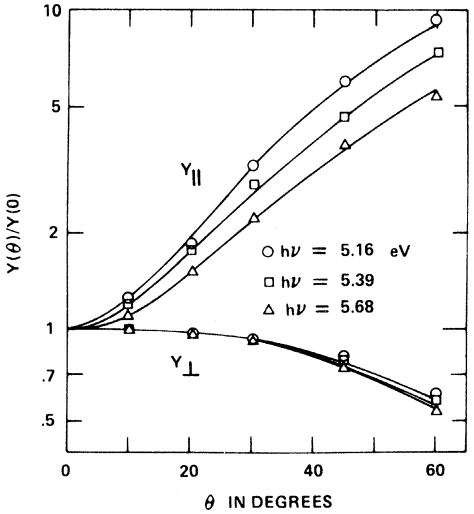

FIG. 1. Angular yield ratios for clean (111) silicon as a function of angle of incidence, obtained for polarization in the plane of incidence $Y_{\parallel}$, and perpendicular to the plane of incidence $Y_{\perp}$. The curves are computed from Eqs. (5) and (6) using the values for r given in the text.

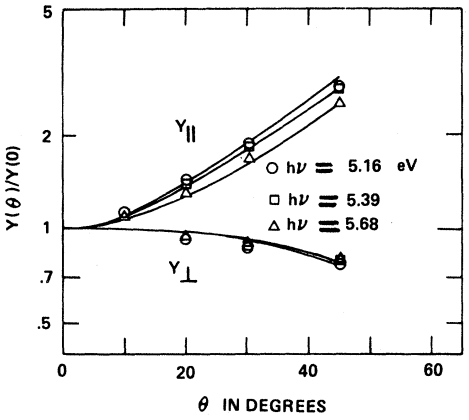

FIG. 2. Angular yield ratios for clean (110) silicon as a function of angle of incidence obtained for polarization in the plane of incidence $Y_{\parallel}$, and perpendicular to the plane of incidence $Y_{\perp}$. The curves are computed from Eqs. (5) and (6) using the values for r given in the text.

in the volume, but they can be perturbed by the presence of the surface in such a manner that enhanced absorption occurs for certain electron states. This viewpoint is supported by several experimental results on silicon and their analyses, which show a large decrease in this absorption with known and controlled modification of the (transition region) surface for a given sample. The experimental results are, to our knowledge, the first such vectorial effects reported on elemental semiconductors and on clean well-categorized single-crystal material, which is, here, silicon in ultrahigh vacuum.

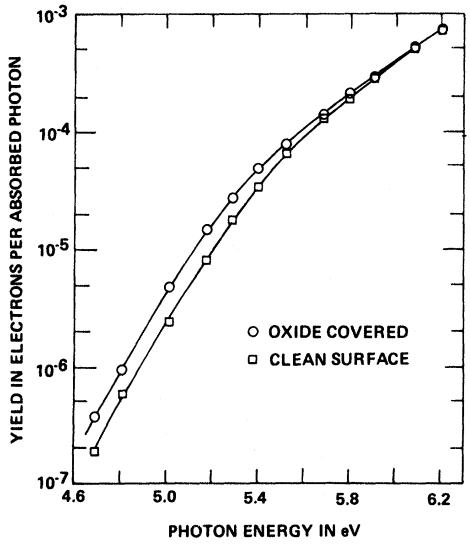

FIG. 3. Photoelectric yields obtained with unpolarized light at normal incidence for (111) silicon with special thin (20–100 Å) oxide layer due to air exposure and with clean surface.

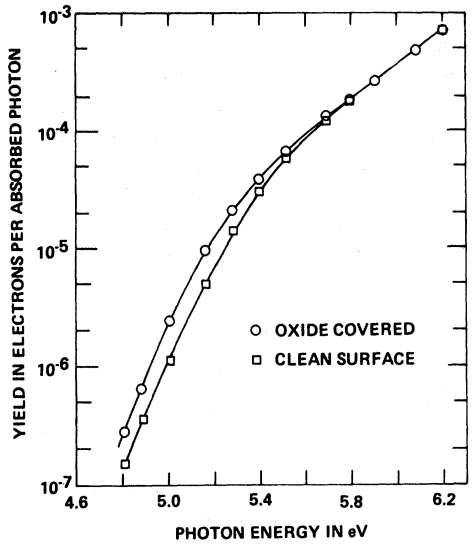

FIG. 4. Photoelectric yields obtained with unpolarized light at normal incidence for (110) silicon with special thin (20–100 Å) oxide layer due to air exposure and with clean surface.

The similarity of some of our silicon results with data of JWJ[24] from molybdenum implies that vectorial photoemission originates from the same basic phenomenon in both metals and semiconductors. If this is so, their vectorial observations could also be attributed to SEOA, and observed sample-to-sample variation would be ascribed to the effects of preparation methods on the (transition region) interface. Since our results are obtained on clean damage-free single crystals, one may eliminate the possibility that previously observed vectorial photoelectric effects are due to volume imperfections within the optical-abosrption depth (about 60 Å in the present uv region for silicon and molybdenum), such as, damage caused by the method of sample preparation or intercrystalline boundaries (which one could be otherwise led to suspect, since the one single-crystal sample investigated by JWJ did not show the vectorial effect). Of course, effects due to imperfections are not ruled out in general.

The existence of SEOA calls for a reexamination and some modification of the present theoretical approach to photoemission, for it essentially specifies that the excitation responsible for observed photoelectrons originates in interaction between electromagnetic energy and extended electron states, whereas most present theory assumes localized excitation. Apparently, the vectorial effect can be theoretically obtained only from approaches such as those now being developed by Schaich and Ashcroft,[26] who derive photoelectric currents from the interaction of the incident electromagnetic field and the electrons in the solid which are in states

determined by their interactions with themselves, the ions, and the surface.

Although the vectorial photoelectric effect is associated with the component of polarization perpendicular to the plane of the surface, it is unlikely that the theoretical modifications suggested by our and JWJ's results will leave untouched the large body of work in the field which has been performed at normal incidence (necessarily with tangential polarization).

II. EXPERIMENTAL PROCEDURES

Experimental arrangements are essentially the same as those described in a previous paper[18] (hereafter referred to as I) except for the utilization of capabilities for rotation of the whole sample-holder assembly about the vertical axis so that the angle of incidence could be varied between $-60°$ and $+60°$. Polarized light was obtained by use of a Glan-Thomson calcite prism, which was rotatable about the direction of incidence. All samples were chosen for perfection and stability by the criteria established in I.

III. EXPERIMENTAL RESULTS

A. Polarized Light, Variable Incidence, and Vacuum Interface

Photoelectric yields were obtained as a function of angle of incidence θ at three wavelengths, for polarization parallel to the plane of incidence $[Y_{\parallel}(\theta)]$ and perpendicular to the plane of incidence $[Y_{\perp}(\theta)]$ for (111) and (110) surfaces as shown in Figs. 1 and 2 normalized to 0° incidence.. Yields were found to be symmetrical about 0° and are therefore shown only for positive angles. The "vectorial effect" is associated with the large increase with angle of incidence of $Y_{\parallel}(\theta)$.

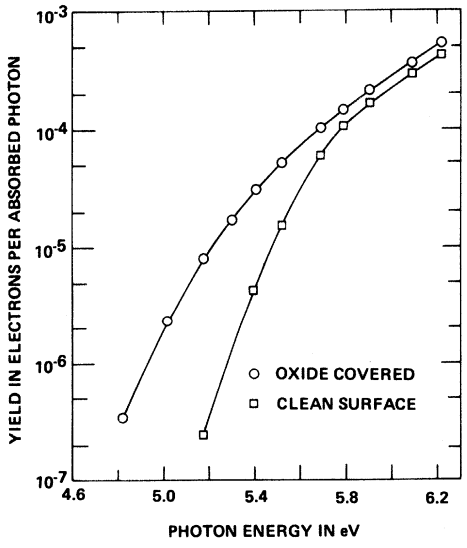

FIG. 5. Photoelectric yields obtained with unpolarized light at normal incidence for (100) silicon with special thin (20–100 Å) oxide layer due to air exposure and with clean surface.

B. Unpolarized Light, Normal Incidence, and Oxide Interface

The essential role played by the interface in the vectorial effect is illustrated in Sec. III C (below) by yields obtained with polarized light from samples covered with the thin oxide layer which occurs because of air exposure (thickness from 20 to 100 Å). Although similar *normalized* vectorial results were found for all oxide-covered silicon, it is more illustrative to consider yields from a special class of such samples: those which had oxide layers which were essentially transparent to photoelectrons emitted from the silicon. Several experimental procedures were found to provide such layers, but the easiest procedure was simply to use samples which were prepared by methods described in I with no special preparation other than the usual 250 °C bake required for ultrahigh vacuum. Use of samples covered with these oxide layers minimizes complications due to scattering in the oxide and provides much larger experimental photocurrents.

The emission of electrons into the vacuum from samples covered with the special oxide layers can be illustrated by photoelectrons which are provided by simple normal-incidence illumination. The elimination of electron loss (in contrast to the usual large decrease in yields observed[17] in most oxide-covered silicon) makes available information about potential barriers on both sides of the oxide, which is also of general interest. Figures 3–5 show yields obtained at normal incidence with unpolarized light for (111), (110), and (100) surfaces covered with these oxide layers for comparison with yields shown for the same samples with the oxides removed (by the usual annealing at 850 °C). Note that *all* (111) and (110) yields are almost identical above about 5.6 eV and that at lower optical energies, oxide-interface yields are *greater* than clean surface yields.

To understand these results, let us recall, as shown in I for vacuum interfaces, that above 5.6 eV all electrons directed toward the surface above the vacuum level will emerge, but that as $h\nu$ decreases, conservation of $\vec{k}_{\parallel}$ across the interface restricts emission to more nearly normal electrons. Using this information, we make the following interpretations: (i) The silicon oxide-vacuum potential barrier is ≈ 4.6 eV, i.e., the same as the (111) and (110) silicon-vacuum barrier but lower than the (100) silicon-vacuum barrier (≈ 4.78 eV). The near identity of *all* high-energy yields shows that oxide-vacuum barriers are almost the same for all orientations, being slightly greater for the (100) sample. The identity of oxide and vacuum yields at higher energies establishes the value of 4.6 eV. (ii) There is negligible loss of electrons by scattering within

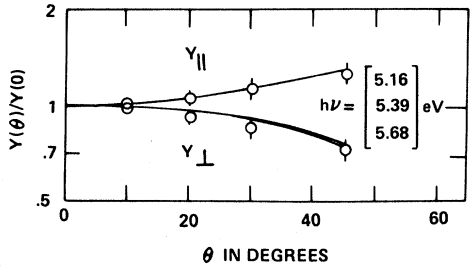

FIG. 6. Angular yield ratios for thin oxide-covered (111) silicon as a function of angle of incidence obtained for polarization in the plane of incidence $Y_{\parallel}$, and perpendicular to the plane of incidence $Y_{\perp}$. The curves are computed from Eqs. (5) and (6) with $r=1$.

the oxide since oxide-covered yields are no smaller than those from vacuum interfaces. (iii) The restrictions on conservation of $\vec{k}_{\parallel}$ have been relaxed or eliminated for the silicon-silicon oxide-vacuum system. The increased yields from oxide-covered surfaces at lower optical energies can be ascribed to the emission of non-normal electrons which would not have been able to emerge through the silicon-vacuum interface because of the requirement for conservation of $\vec{k}_{\parallel}$ across the interface (see Sec. VI of I for discussion of this point). This viewpoint is consistent with estimates which show that observed oxide-surface yields are no greater than the maximum possible if all electrons at all directions could emerge (escape angle always is 90°) below 5.6 eV as well as above. (iv) The silicon-silicon oxide barrier ≤ 4.6 eV; otherwise some of the emission would be cut off.

Therefore, it has been shown that for $h\nu \geq 5.6$ eV, one collects all electrons excited in the silicon for *both* oxide and vacuum interface systems (directed toward the surface, of course); and for $h\nu \leq 5.6$ eV, one collects at least as many of the excited electrons for the oxide-covered surface. Thus, the effective difference for photoemission between special oxide-covered samples and clean-surface samples is that

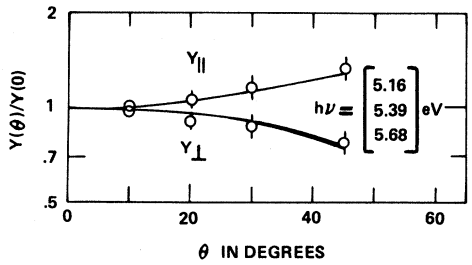

FIG. 7. Angular yield ratios for thin oxide-covered (110) silicon as a function of angle of incidence obtained for polarization in the plane of incidence $Y_{\parallel}$ and perpendicular to the plane of incidence $Y_{\perp}$. The curves are computed from Eqs. (5) and (6) with $r=1$.

the interface is silicon-silicon oxide, in one case, and silicon-vacuum, in the other. With this understanding, the remarkable role played by the interface in the vectorial effect can be seen in the following data.

C. Polarized Light, Variable Incidence, and Oxide Interface

Photoelectric yields were obtained as a function of angle of incidence at the same three wavelengths for both parallel and perpendicular polarization for (111) and (110) oxide-covered surfaces, as shown in Figs. 6 and 7 normalized to 0° incidence. These are to be compared with Figs. 1 and 2.

Note that yield ratios for perpendicular polarization are essentially identical to those from vacuum interfaces. But yield ratios for parallel polarization are *much smaller*. The vectorial effect is greatly diminished; in fact, it will be shown that, within experimental error, it has completely vanished.

D. Unpolarized Light, Variable Incidence, and Vacuum Interface

Since $Y_{\parallel}(\theta)$ is larger than $Y_{\perp}(\theta)$ in Figs. 1 and 2, it would be expected that yields obtained at variable incidence with *unpolarized* light [defined simply as $Y(\theta)$] would increase with θ. In fact, we have verified by experimental measurements on several samples that the simple average applies:

$$Y(\theta) = \tfrac{1}{2}[Y_{\parallel}(\theta) + Y_{\perp}(\theta)] , \qquad (1)$$

as required by the cubic symmetry of the material. Thus, a useful measure of vectorial effects can be

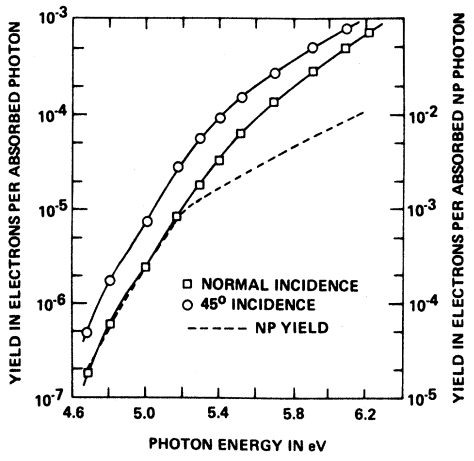

FIG. 8. Photoelectric yields from (111) silicon. Measured yields per total absorbed photon obtained with unpolarized light at 0° and 45° incidence associated with the ordinate on the left-hand side of figure. Computed yield per absorbed normally polarized photon using these measured yields and Eq. (7) is shown by dashed line associated with the ordinate on the right-hand side of figure. Note that the scale is 100 times larger, thus these yields are much greater.

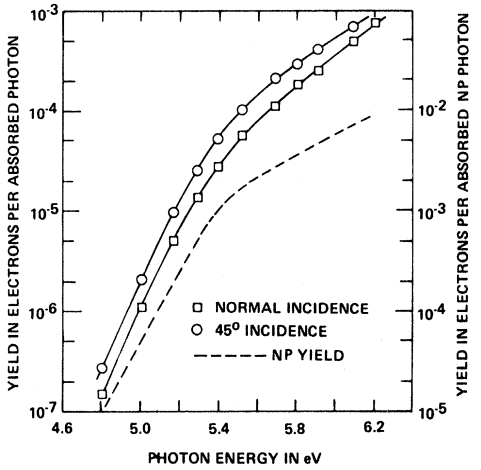

FIG. 9. Photoelectric yields from (110) silicon. Measured yields per total absorbed photon obtained with unpolarized light at 0° and 45° incidence associated with the ordinate on the left-hand side of figure. Computed yield per absorbed normally polarized photon using these measured yields and Eq. (7) is shown by dashed line associated with ordinate on the right-hand side of figure. Note that the scale is 100 times larger, thus these yields are much greater.

obtained simply by measurement of $Y(\theta)$. A convenient procedure is to measure yields at 45° [$Y(45)$] for comparison with yields at 0° [$Y(0)$]. The experimental results for $Y(45)$ and $Y(0)$ over the full spectral range are shown in Figs. 8–10 for (111), (110), and (100) surfaces, respectively. The dashed curves in the figures will be discussed later.

Note that the differences between $Y(45)$ and $Y(0)$ are large and readily measurable. Moreover, they turn out to be a complete measure of the vectorial effect for this system since, as will be seen later, $Y_\perp(\theta)$ can be obtained from known optical parameters. Figures 8.—10 indicate the continuity of vectorial yields over the whole spectral range.

E. Unpolarized Light, Variable Incidence, and Oxide Interface

It was found, as would be expected from Eq. (1) and Figs. 6 and 7, that over the whole spectral range, $Y(45) \approx Y(0)$. The results of large numbers of observations on many samples permitted the determination that $Y(45)$ is on the average about 1 to 2% larger than $Y(0)$.

IV. INTERPRETATION AND ANALYSIS

A. Basic Viewpoints

We present here an analysis which is consistent with all experimental results and which phenomenologically indicates that the basic process underlying the vectorial effect is SEOA. The analysis is based on the following viewpoints:

(i) The optical energy in the volume can be determined from classical electromagnetic theory, and thus can be calculated anywhere in the system for any angle of incidence using only known values of the complex index of refraction $n+ik$. This has been recognized and implemented by Fan[7] and JWJ.[24] Electromagnetic radiation, with propagation vector $\vec{\kappa}$ and specified polarization, is incident upon the medium which, being polarizable, interacts with the radiation within a short distance of the interface d_s to set up new values for $\vec{\kappa}$ and new phase relations. It has been recognized for many years[7,27,28] that d_s is less than a few angstroms. Hence, it is much smaller than the presently applicable optical absorption distance of about 60 Å, and classical electromagnetic theory is applicable to most of the medium.

(ii) In this system, the optical energies are determined not by the operant excitations (those leading to photoemission), but by the far greater amount of optical absorption due to excitations which terminate below the vacuum level. This is easily seen both from observation of the band structure and from the fact that photocurrents become several orders of magnitude larger when barrier heights are lowered by the application of cesium.[29] These transitions then determine the optical properties of the material, which in turn determine the electromagnetic energies in the volume.

(iii) Observed photoelectric yields are directly related to the optical absorption *due to the operant transitions* in the volume. This viewpoint must be considered as an ansatz to be supported by experi-

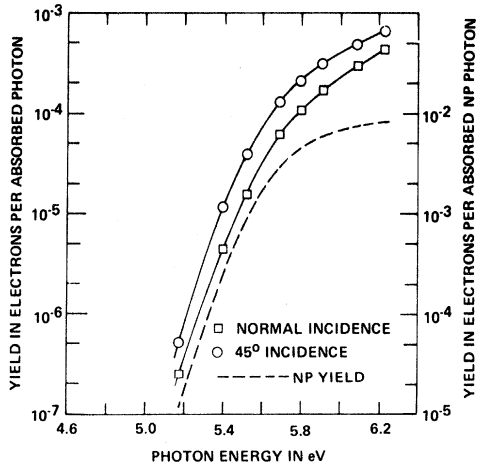

FIG. 10. Photoelectric yields from (100) silicon. Measured yields per total absorbed photon obtained with unpolarized light at 0° and 45° incidence associated with the ordinate on the left-hand side of figure. Computed yield per absorbed normally polarized photon using these measured yields and Eq. (7) is shown by dashed line associated with the ordinate on the right-hand side of figure. Note that the scale is 100 times larger, thus these yields are much greater.

mental yields for all polarizations and angles of incidence. It is suggested by the extensive information on photoelectric emission excited by normal-incidence illumination: Scattering, emission, and transport effects, if present, do not change with the intensity of illumination. Hence, for a fixed value of $h\nu$, yields will be proportional to optical excitation. For silicon, it is possible to broaden this viewpoint, since it has been shown in I[18] that, in the present energy range, there is negligible loss of electrons due to scattering. Moreover, above $h\nu \cong 5.6$ eV, the escape angle approaches 90°, and therefore photocurrents are proportional to $\frac{1}{2}$(optical absorption due to *all* electrons excited above the vacuum level); below 5.6 eV, the escape angle narrows, and the constant of proportionality becomes a function of $h\nu$.

B. Basic Ansatz

Taking the internal excitation approach of JWJ, let $E_{TP}(\theta)$ be the electromagnetic energy within the solid which is associated with the electric vector parallel to the plane of the surface (TP stands for "tangential polarization"), and let $E_{NP}(\theta)$ be the same for light which is polarized perpendicular to the surface (NP stands for "normal polarization"). The basic ansatz is that all yields are due only to excitations within the volume and are thus generated by, and proportional to, $E_{TP}(\theta)$ and $E_{NP}(\theta)$, which can be treated independently, but which are not necessarily equally effective in causing optical excitations. Letting the effectiveness in causing optical excitations be proportional to α and β, respectively, any yield can be written

$$Y'(\theta) = \alpha E_{TP}(\theta) + \beta E_{NP}(\theta) \tag{2}$$

or

$$Y'(\theta) = \alpha[E_{TP}(\theta) + r E_{NP}(\theta)] \,. \tag{3}$$

The ratio $r(=\beta/\alpha)$ is essentially the parameter B used by JWJ, which our results suggest is associated with SEOA. The vectorial effect occurs when B, or r, which can be called the "enhancement ratio," is greater than 1. Comparison is made with experimental angular ratios, so that we use the following form of Eq. (3):

$$\frac{Y'(\theta)}{Y'(0)} = \frac{E_{TP}(\theta)}{E_{TP}(0)} + r\,\frac{E_{NP}(\theta)}{E_{TP}(0)} \,, \tag{4}$$

since $E_{NP}(0) = 0$. By experimentally changing the angle of incidence for known polarization, $E_{TP}(\theta)/E_{TP}(0)$ and $E_{NP}(\theta)/E_{TP}(0)$ are made to vary in a definite manner with θ, which can be calculated from classical electromagnetic theory. If the ansatz is correct, then it is necessary that Eq. (3) hold with r being constant, i.e., independent of θ; if SEOA is applicable, then r will depend only on the condition of the interface (for a given material and crystalline orientation).

The following coordinate system is used. The z direction is normal to the plane of the surface, and x and y are tangential to the plane of the surface. The plane of incidence is the yz plane and the angle of incidence θ is, therefore, the angle between the direction of incidence and the z direction. $E_x(\theta)$ represents the electromagnetic energy in the solid associated with the electric vector polarized in the x direction, and similarly for y and z. When the incident light is polarized perpendicular to the plane of incidence, the polarization vector remains in the plane of the surface and there is no NP component. Hence, Eq. (4) becomes

$$\frac{Y_\perp(\theta)}{Y_\perp(0)} = \frac{E_x(\theta)}{E_x(0)} \,, \tag{5}$$

and for polarization parallel to the plane of incidence, it becomes

$$\frac{Y_\parallel(\theta)}{Y_\parallel(0)} = \frac{E_y(\theta)}{E_y(0)} + r\,\frac{E_z(\theta)}{E_y(0)} \,. \tag{6}$$

Energy ratios on the right-hand sides of Eqs. (5) and (6) were calculated from classical electromagnetic theory, as shown in the Appendix, and were compared with the experimental yield ratios shown in Figs. 1, 2, 6, and 7 for (111) and (110) samples with both vacuum and oxide interfaces. When this was done, it was indeed found, in support of the ansatz, that Eqs. (5) and (6) were satisfied for all samples, clean and oxide covered, and at all wavelengths, with r independent of θ, as required.

For the *oxide-interface* samples, all yield ratios (NP and TP) were found to be directly proportional to energy ratios in the solid, since Eq. (6) was found to be satisfied with $r = 1$ (which we have established on many samples) for all $h\nu$ and all crystalline orientations. Thus, yield ratios are proportional to the ratios of energy absorbed in the solid and equal to $[1 - R(\theta)]/[1 - R(0)]$, where $R(\theta)$ and $R(0)$ are reflectances for either the parallel or perpendicular case, i.e., if yield ratios shown in Figs. 6 and 7 were expressed in terms of absorbed energy ratios *at each angle* of incidence, then all curves would be straight lines of value equal to 1.

For the *vacuum interface*, Eq. (6) was satisfied for much larger values of r(independent of θ, as required), which were, for the (111) sample, $r = 94$, 70, and 44, at $h\nu = 5.16$, 5.39, and 5.68 eV, respectively; for the (110) sample, $r = 35$, 33, and 24 (all ± 5) for the same photon energies.

These results are illustrated in Figs. 1, 2, 6, and 7 by comparison of experimental data with curves computed from energy ratios in Eqs. (5) and (6) using the above values of r.

It is the comparison between vacuum- and oxide-

interface samples that phenomenologically suggests SEOA. All oxide-interface yields are simply proportional to energies in the volume (i.e., $\alpha=\beta$, thus $r=1$), and there is no enhancement. Then, when nothing is changed except conditions at the interface (same sample, same orientation, etc.,), yields for the vacuum interface due to NP photons are greatly increased, and yields due to TP photons remain unchanged, while both remain independently proportional to energy ratios in the volume. Furthermore, we have found that upon increasing exposure of the clean surface to oxygen, beginning with fractional monolayer amounts, the degree of enhancement decreases continuously from its clean-surface value towards zero ($r\to 1$).

C. Determination of r throughout the Spectral Region

The enhancement ratio can also be determined from yield ratios measured with unpolarized light because of the applicability of Eq. (1) to this system. Using Eqs. (1), (5), and (6), we find

$$r=\left(\frac{E_y(0)}{E_z(45)}\right)\left(\frac{2Y(45)}{Y(0)}-\frac{E_x(45)+E_y(45)}{E_y(0)}\right) . \qquad (7)$$

Remembering the definition of r, Eq. (7) enables the easy determination of spectral yields per absorbed NP *photon* from the data shown in Figs. 8–10, for $Y(0)$ and $Y(45)$ as a function of $h\nu$. The results of this computation for clean-surface samples are also displayed in Figs. 8–10. Note the continuity and *much greater efficiency* of NP yields over the complete spectral range.

V. DISCUSSION

A. Volume Absorption

The considerations of Sec. IV have shown that yields for both NP and TP illumination are proportional to energies in the volume (i.e., inside the optical-transition distance d_s). However, they alone cannot specify the depth from which operant electrons originate. This is because, as shown by JWJ (see Appendix of this paper) energy *ratios* depend very weakly on distance within the solid. For example, the possibility must be considered that NP photoelectrons (those generated by NP radiation) could originate from surface states just inside d_s.

Evidence which indicates that NP photoelectrons are due to the same processes as TP electrons, and thus originate well within the volume optical-absorption distance, can be deduced from inspection of the spectral dependences shown in Figs. 8–10 for both NP and TP illumination. Let us recall that extensive work at normal incidence (necessarily TP) has related photoelectric yields and energy distributions to volume band structures. Therefore, it is well-established that TP yields are determined by (i) transition probabilities and (ii) densities of state in (iii) the band structure; and spectral dependences of the yield are determined by (iv) variation with $h\nu$ of available densities of state and variations with $h\nu$ of the escape angle (which depends on conservation of $\vec{k}_{\parallel}$ across the boundary). Now, all effects (i)–(iv) depend on specific volume properties of the material. Thus, the almost identical spectral dependences of NP and TP yields at lower energies (although the former are much more efficient) strongly suggest that photoelectrons excited by NP radiation also originate in the volume, although their excitation is affected by the interface. Similar evidence for volume optical absorption can be drawn for molybdenum from the observation of JWJ (shown in their Fig. 7) that spectral dependences of the yield were independent of angle of incidence for polarization parallel to the plane of incidence.

In view of this discussion and viewpoint (iii) of Sec. IV A, which indicate that transport effects are absent, we are led to propose that the vectorial effect is due *only* to optical absorption in the volume of NP radiation; but this absorption is strongly influenced by the condition of the surface. Note that the pertinent absorption is related *only* to the operant excitations which, by viewpoint (ii) of Sec. IV A, represent only a small fraction of the total.

B. Crystallographic Vectorial Effects

Effects of crystal symmetry on optical absorption must be considered. Selection rules for absorption of light in crystalline media predict strong dependence of excitation probabilities on the direction of polarization for electrons with crystal momentum $\vec{k}$ in symmetry directions.

Qualitative theoretical predictions and confirming experimental results of such effects were presented by Gobeli, Allen, and Kane[30] using normally incident polarized light on (111) silicon in experiments which showed large variations in photocurrents of electrons emerging in ⟨110⟩ and ⟨112⟩ symmetry directions as the angle of polarization was rotated in the plane of the surface.

For illumination at variable angle of incidence θ, it has been shown by Gourary[31] from group theoretical considerations that transition probabilities for electrons with $\vec{k}$ in ⟨111⟩, ⟨110⟩, or ⟨100⟩ directions will go either as $\sin^2(\theta)$ or as $\cos^2(\theta)$ depending on the symmetry of the wave functions for the operant transitions. When $\vec{k}$ is not in a symmetry direction, the relations are more complicated, and no simple relation is to be expected.

Selection rules must be considered in general, but they can be ruled out as the source of our vectorial observations (and presumably those of JWJ and others as well) for several reasons, the most direct being our observations of the influence of the surface, which is not encompassed in volume selection rules (in a broader sense, SEOA might be thought

of as a surface-volume–determined selection rule). In addition, previous work on this system (I[18]) has shown that the escape angle becomes quite large for $h\nu$ only a few tenths of an eV above threshold, and therefore, observed yields can originate from electrons over a large solid angle, thus decreasing symmetry effects. (Note, for example, that all effects of crystal symmetry must disappear at an escape angle of 90°, since the total excitation of cubic systems is independent of direction of polarization.) We have substantiated these conclusions in experiments performed with polarized light normally incident on (110) silicon in which the *yield* was found to be independent of the direction of polarization in the plane of the surface; if selection rule effects were important, then anisotropy of the yield would have been observed.

Volume vectorial effects have also been investigated by Puff[32] in theories of photoemission, based on a quasi-free-electron model, which predict excitation probabilities proportional to $|\hat{e}\cdot\vec{G}|^2$, where $\hat{e}$ is the direction of polarization and $\vec{G}$ is a reciprocal-lattice vector. These effects can also be ruled out as the source of our observations for the same reasons as above.

It can be speculated that the observed dependences of r on crystal orientation could be related to the possibility that SEOA would be a maximum for electrons with $\vec{k}$ normal to the surface, and decrease as $\vec{k}$ moves away from the normal. This is consistent with results presented in I which showed qualitatively that at lower optical energies, the (111) sample has the largest normal component of $\vec{k}$, the (100) has less, and the (110) least of the three; in agreement with differences in NP yields shown in Figs. 8–10 and in parallel yields shown in Figs. 1 and 2. At higher optical energies, when the excitation becomes almost completely isotropic, NP yields should approach the same value for all orientations, as observed. In this context, the noticeable change in slope of yields near 5.6 eV would occur because the escape angle becomes very close to 90°, so that large numbers of presumably less-effective nearly tangential electrons can emerge.

C. Source and Significance of SEOA in Photoemission

It is evident that the existence of SEOA requires some modification and extension of present theories of photoemission, most of which are based on localized excitation (for example, see Berglund and Spicer[20]). To illustrate: If the yield formula of Sec. IV had been considered in context of these theories, Eqs. (2) and (3) could have been expressed as

$$Y_\perp(\theta)\propto\int_0^\infty|\mathcal{E}_x(z,\theta)|^2X(z)P(z)\,dz\ , \tag{8}$$

$$Y_\parallel(\theta)\propto\int_0^\infty|\mathcal{E}_y(z,\theta)|^2X(z)P(z)\,dz$$

$$+\int_0^\infty|\mathcal{E}_z(z,\theta)|^2X'(z)P'(z)\,dz\ , \tag{9}$$

where $\mathcal{E}_y(z,\theta)$ is the amplitude of the component of the electric field in the y direction as a function of depth and angle of incidence; and similarly for the x and z directions. $X(z)$ represents the total excitations per unit field at the depth z which terminate above the vacuum level, and $P(z)$ is an escape function which designates the fraction of electrons excited at depth z which eventually emerge into the collecting medium, both referring to tangential polarization; $X'(z)$ and $P'(z)$ represent the same operations for normal polarization. Note, for completeness, that the following relation is applicable to $\mathcal{E}_x(z,\theta)$:

$$|\mathcal{E}_x(z,\theta)|=|\mathcal{E}_x(z=0,\theta)|e^{-\alpha(\theta)z}\ , \tag{10}$$

and similarly for y and z, where $\alpha(\theta)$ is the absorption coefficient, which depends only weakly on θ.

If one attempts to apply such a local theory to include SEOA, differences in effectiveness of normal and tangential illumination in generating photoelectrons would have to originate in possible differences between $X(z)P(z)$ and $X'(z)P'(z)$. If only known physical mechanisms are considered, $X(z)$ cannot depend on z since it is a volume excitation, and there remains only the possibility of volume crystallography effects, which have been eliminated above. Otherwise, *ad hoc* dependences of $X(z)$ and $P(z)$ on z and on polarization would be required. Thus, the need is indicated for a theory based on excitation of extended electron states, such as that of Schaich and Ashcroft,[26] which is discussed in the Introduction.

For other theoretical suggestions, it may be possible that the appearance of SEOA depends on the mean free path of the *operant* electrons being larger than, or the order of, the optical-absorption depth (which has been shown for this system[18]). Hence, it could be a high-energy analog to the well-known anomalous skin effect,[33] which has been observed in metals and derived for the quite different situation of a free-electron gas at low photon energies (intraband rather than interband transitions) by necessarily nonlocal theories. In addition, Stern[34] has discussed anomalous absorptions in alkali metals, and has shown[35] that if electron scattering at the interface is specular, $\vec{k}$ conservation requires mixing and changing of electron states within a mean free path, although this model was also illustrated only for a nearly free-electron gas.

D. Applications

The considerations of this paper indicate that the vectorial effect originates in SEOA, and thus depends on electron states near interfaces. Thus, photoelectric experiments, such as those reported here, can provide information not only about these

states, but about the interface itself, as shown by our results upon exposure of the clean surface to oxygen gas.

ACKNOWLEDGMENTS

The author wishes to express his appreciation for the assistance of V. Failla, who took most of the data, and to Dr. B. Burdick for the computer calculation of the energy ratios.

APPENDIX

Energy relations are available from classical electromagnetic theory, which we have used differently than JWJ in some respects. The coordinate system is described in Sec. IV. The total energy absorbed [and, hence, available for excitation of operant electrons—see Sec. IV A (ii)] is obtained from reflectances[36] which, using the terminology of JWJ, are given by

$$R_{\parallel}(\theta)=\left|s_0^2\cos\theta-s\right|^2/\left|s_0^2\cos\theta+s\right|^2, \tag{A1}$$

$$R_{\perp}(\theta)=\left|s-\cos\theta\right|^2/\left|s+\cos\theta\right|^2, \tag{A2}$$

where

$$s\equiv(s_0^2-\sin^2\theta)^{1/2},\quad s_0=n+ik, \tag{A3}$$

and $R_{\parallel}(\theta)$ and $R_{\perp}(\theta)$ are the reflectances for illumination with polarization parallel and perpendicular to the plane of incidence, respectively.

Also required are the components of the electric field just inside the surface optical-transition distance d_s which have been derived, e.g., by Fan[7]

$$\mathcal{E}_x/\mathcal{E}_i=2\cos\theta/(s+\cos\theta), \tag{A4}$$

$$\mathcal{E}_y/\mathcal{E}_i=2s\cos\theta/(s+s_0^2\cos\theta), \tag{A5}$$

$$\mathcal{E}_z/\mathcal{E}_i=2\sin\theta\cos\theta/(s+s_0^2\cos\theta). \tag{A6}$$

The $\mathcal{E}_x$ is the (complex) component of the electric field just inside the surface in the x direction, and similarly for y and z. The $\mathcal{E}_i$ is the amplitude of the incident field.

One wishes to calculate two types of angular ratios (quantities normalized to 0° angle of incidence): total energy ratios and ratios of electric fields just inside the medium.

Let $E_x^t(\theta)$ be the *total* energy absorbed within the medium which corresponds to electromagnetic radiation with the component of polarization in the x direction, and similarly for y and z. Since the electric vector remains in the plane of the surface at all angles of incidence when it is perpendicular to the plane of incidence, $R_{\perp}(\theta)$ determines $E_x^t(\theta)$ directly. But polarization parallel to the plane of incidence contains components in both the y and z directions for which one must determine energies independently. This information can be provided from the components of the electric vectors just inside the surface. Although amplitudes decrease, relative phases and magnitudes remain unchanged as energy propagates into the medium, so that we can write

$$\rho_x^t\equiv\frac{E_x^t(\theta)}{E_x^t(0)}=\frac{1-R_{\perp}(\theta)}{1-R_{\perp}(0)}, \tag{A7}$$

$$\rho_y^t\equiv\frac{E_y^t(\theta)}{E_y^t(0)}=\frac{1-R_{\parallel}(\theta)}{1-R_{\parallel}(0)}\,\frac{|\mathcal{E}_y(\theta)|^2}{|\mathcal{E}_y(\theta)|^2+|\mathcal{E}_z(\theta)|^2}, \tag{A8}$$

$$\rho_z^t\equiv\frac{E_z^t(\theta)}{E_y^t(0)}=\frac{1-R_{\parallel}(\theta)}{1-R_{\parallel}(0)}\,\frac{|\mathcal{E}_z(\theta)|^2}{|\mathcal{E}_y(\theta)|^2+|\mathcal{E}_z(\theta)|^2}. \tag{A9}$$

Electric field intensity ratios are calculated from (A4)–(A6). Then dividing by $\cos\theta$ for proper area relations we have

$$\rho_x^m\equiv\frac{1}{\cos\theta}\,\frac{|\mathcal{E}_x(\theta)|^2}{|\mathcal{E}_x(0)|^2}=\cos\theta\,\frac{|1+s_0|^2}{|s+\cos\theta|^2}, \tag{A10}$$

$$\rho_y^m\equiv\frac{1}{\cos\theta}\,\frac{|\mathcal{E}_y(\theta)|^2}{|\mathcal{E}_y(0)|^2}=\cos\theta\,\frac{|s|^2|1+s_0|^2}{|s+s_0^2\cos\theta|^2}, \tag{A11}$$

$$\rho_z^m\equiv\frac{1}{\cos\theta}\,\frac{|\mathcal{E}_z(\theta)|^2}{|\mathcal{E}_y(0)|^2}=\sin^2\theta\cos\theta\,\frac{|1+s_0|^2}{|s+s_0^2\cos\theta|^2}. \tag{A12}$$

Values of n and k for silicon can be obtained from Eden,[37] and are also available in graphical form from Philip and Taft.[38]

It is important to determine the dependence of energy ratios on the depth from which operant electrons originate, as shown by JWJ. If they are produced just inside the surface optical-transition distance d_s, then yield ratios would be determined by intensity ratios of the electric fields shown in Eqs. (A10)–(A12). If they are produced throughout the complete optical-absorption depth, then yield ratios would be determined by the total energy ratios shown in Eqs. (A7)–(A9). Comparison between these two possibilities by straightforward calculation gives

$$\rho_x^t/\rho_x^m=\mathrm{Res}/\mathrm{Res}_0, \tag{A13}$$

$$\frac{\rho_y^t}{\rho_y^m}=\frac{\rho_z^t}{\rho_z^m}=\frac{\mathrm{Re}(s^*s_0^2)}{\mathrm{Res}_0}\,\frac{1}{|s|^2+\sin^2\theta}. \tag{A14}$$

For the values of n and k applicable to these systems (e.g., $n=1.30$ and $k=3.00$ for silicon at 5.68 eV), the quantities in Eqs. (A13) and (A14) deviate no more than a few percent from a value of 1 at all angles of incidence. Hence, in agreement with JWJ, we see that one cannot readily distinguish the depth from which photoelectrons originate by yield ratio measurements alone—additional criteria are needed.

*Present address: 11 Camelot Drive, Bloomfield, Conn.
[1]K. Mitchell, Proc. Roy. Soc. (London) A146, 442 (1934); A153, 513 (1935).
[2]R. E. B. Makinson, Proc. Roy. Soc. (London) A162, 367 (1937); Phys. Rev. 75, 1908 (1949).
[3]M. J. Buckingham, Phys. Rev. 80, 704 (1950).
[4]I. Adawi, Phys. Rev. 134, A788 (1964); 134, A1649 (1964).
[5]J. Elster and H. Geitel, Ann. Phys. (Leipzig) 52, 433 (1894); 55, 684 (1895); 61, 445 (1897).
[6]H. Ives, Astrophys. J. 60, 209 (1924); 60, 231 (1924); Phys. Rev. 38, 45 (1931).
[7]H. Y. Fan, Phys. Rev. 68, 43 (1945).
[8]H. Thomas, Z. Physik 147, 395 (1957).
[9]H. Mayer and H. Thomas, Z. Physik 147, 419 (1957).
[10]S. Methfessel, Z. Physik 147, 442 (1957).
[11]A. Meesen, J. Phys. Radium 22, 135 (1961); 22, 308 (1961); Phys. Status Solidi 26, 125 (1968).
[12]L. Apker, E. Taft, and J. Dickey, Phys. Rev. 74, 1462 (1948).
[13]D. Redfield, Phys. Rev. 124, 1809 (1961).
[14]J. J. Scheer, Philips Res. Rept. 15, 584 (1960).
[15]W. E. Spicer, J. Appl. Phys. 31, 2077 (1960); RCA Rev. 19, 555 (1958).
[16]G. W. Gobeli and F. G. Allen, Phys. Rev. 127, 141 (1962); 127, 150 (1962).
[17]F. G. Allen and G. W. Gobeli, J. Appl. Phys. 35, 597 (1964).
[18]R. M. Broudy, Phys. Rev. B 1, 3430 (1970).
[19]For recent references on semiconductors, see, also, T. E. Fischer, Surface Sci. 13, 30 (1969).
[20]C. N. Berglund and W. E. Spicer, Phys. Rev. 136, A1030 (1964); 136, A1044 (1964).
[21]For recent references on metals, see, also, D. H. Seib and W. E. Spicer, Phys. Rev. B 2, 1676 (1970); 2, 1694 (1970).
[22]M. Brauer, Phys. Status Solidi 14, 413 (1966).
[23]G. Frischmuth-Hoffman, P. Görlich, H. Hora, W. Heimann, and H. Marseille, Z. Naturforsch. 15a, 648 (1960).
[24]D. W. Juenker, J. P. Waldron, and R. J. Jaccodine, J. Opt. Soc. Am. 54, 216 (1964).
[25]A preliminary account has appeared elsewhere (unpublished).
[26]W. L. Schaich and N. W. Ashcroft, Solid State Commun. 8, 1959 (1970).
[27]L. I. Schiff and L. H. Thomas, Phys. Rev. 47, 860 (1935).
[28]G. D. Mahan and G. Obermaier, Phys. Rev. 183, 834 (1969).
[29]G. W. Gobeli and F. G. Allen, Phys. Rev. 144, A558 (1966).
[30]G. W. Gobeli, F. G. Allen, and E. O. Kane, Phys. Rev. Letters 12, 94 (1964).
[31]B. S. Gourary (private communication).
[32]H. Puff, Phys. Status Solidi 1, 636 (1961); 1, 704 (1961); 4, 125 (1964); 4, 365 (1964); 4, 569 (1964).
[33]For a recent derivation and reference to previous work, see J. G. Collins, Appl. Sci. Res. B7, 1 (1957).
[34]E. A. Stern, in *Proceedings of the Fourth International Materials Symposium*, edited by G. A. Somorjai (Wiley, New York, 1969).
[35]E. A. Stern, Phys. Rev. 162, 565 (1967).
[36]J. A. Stratton, *Electromagnetic Theory* (McGraw-Hill, New York, 1941), Chap. 9.
[37]R. C. Eden, Ph. D. thesis (Stanford University, 1967) (unpublished).
[38]H. R. Philip and E. A. Taft, Phys. Rev. 120, 37 (1960).

PHYSICAL REVIEW B VOLUME 3, NUMBER 11 1 JUNE 1971

Electron Paramagnetic Resonance of Coupled Spin Systems: $Gd_xZr_{1-x}Zn_2$

D. Davidov,* G. Dublon, and D. Shaltiel†
Department of Physics, Hebrew University, Jerusalem, Israel
(Received 25 August 1970)

The electron paramagnetic resonance (EPR) of the coupled spin system $Gd_xZr_{1-x}Zn_2$ was measured as a function of the temperature T and the Gd concentration x. By varying x and T we were able to vary the relaxation parameters in a systematic way and obtain appreciable variation of both the EPR g shift and linewidth. We succeeded in correlating the variation of the relaxation parameters with the modified Hasegawa model. This is the first time that such a correlation has been obtained in a nonbottlenecked system.

The dynamic and static behavior of conduction electrons and paramagnetic ions coupled by exchange interactions is a subject of considerable interest. Hasegawa[1] was the first to suggest that these coupled spin systems may be described by phenomenological Bloch-type equations. The solutions of Hasegawa's equations give the transverse susceptibility as well as the electron paramagnetic resonance (EPR) g shift and linewidth of both the paramagnetic ions and conduction electrons. These solutions also indicate the existence of the well-known "bottleneck" effect[2] and dynamic effects.[3] In the past few years these problems have been studied extensively both theoretically[4] and experimentally.[5] There exists experimental studies that confirm Hasegawa's theory.[2,5,6] Most of these studies are concerned with the CuMn system and in the extreme bottleneck regime. $LaNi_5$[7] is somewhat exceptional in that the variation of the g shift arises from dynamic effects. However, as yet